STRUCTURAL DESIGN FOR A 3DOF ROBOT LOWER-ARM VIA COMPUTER AIDED ENGINEERING

Choong W. H. & Yeo K. B.

Centre of Materials & Minerals, Universiti Malaysia Sabah
88999 Kota Kinabalu, Sabah, Malaysia.

ABSTRACT. *This paper described a design and analysis of a lower arm structure of a 3DoF robot arm capable of 6kg payload and with a workspace envelope radius of 1.3m. The lower arm structure is designed with the advantage to improve the system efficiency and accuracy. The structure is designed with selected material and geometric properties, which allows the system repeatability to improve from ±0.1mm to ±0.0705mm. A systematic sequence of design material selection and cross-section dimension identification has been introduced to enhance the design process efficiency. The final result on material selection and dimensional properties of the structure is then preceded with computer aided engineering analysis*.

KEYWORDS. Structural Design, Robot Lower-Arm, Material Modeling, CAE.

INTRODUCTION

A three degree of freedom (DoF) articulated robot arm consists of three linkages, which compromises of a base, lower arm and upper arm. Each linkage has its own structure design, characteristic, and function to enhance as a complete robot arm formation. Linkage structure design plays a very important role in defining the robot arm efficiency and flexibility. Ideally designed and optimized structures are able to support the efficiency of joint actuators and prolonging the robot arm operating life span.

The lower arm structure has the most critical structure comparing to the upper arm and the base. In the case of a robot arm of a serial articulate manipulator, therefore, the lower arm structure must be designed to have the ability to handle the robot payload and the total weight of upper arm and wrist mechanisms. While the load that acts on the lower arm will not affect the base structure due to base joint axis being perpendicular to the lower arm (shoulder) joint axis.

To achieve the efficiency and maneuverability, lower arm structure is required to be designed in high specific stiffness (stiffness/density ratio) (Kim, *et. al.*, 1996). High specific stiffness has the ability of resisting deflection that occurs as the design payload is applied. In general, the structure stiffness (k) can be identified as the ratio between the applied load (P) and maximum deflection (δ_{max}) that occurs as a result of the applied load; if the axial loadings are negligible.

Structure stiffness, $$k = \frac{P}{\delta_{max}} \quad (1)$$

The solution of structural deflection with the flexural rigidity constant along the length can be defined as,

$$EI \frac{d^2\delta}{dx^2} = M(x) \tag{2}$$

Such that,

E	-	the material's modulus of elasticity
I	-	the beam structure's moment inertia computed about the neutral axis
M	-	the internal moment in the beam structure at the x been measured
x	-	a distance of the overall length of the beam structure

Others parameters such as structural geometry and material are also required to be considered in robot arm link structure design, in order to avoid or prevent design performance failure.

Linkage structure deflection occurrences will deficient the robot system efficiency whereby deflection can create positioning errors as the robot repeats the positioning tool-tip to the previous taught point. This positioning error is commonly known as position accuracy or repeatability. Repeatability error can also affect the joint actuator, and the power transmission stiffness (Schilling & Groover., 1990). Currently, the available industrial robots can achieve the repeatability of ±0.08mm to ±0.5mm with respect to their maximum payload (Lewis, *et. al.*, 2005). Repeatability error can be eliminate or reduce by increasing the robot structure stiffness, structural design and material properties controls the stiffness limitation. Deflection compensation can be introduced into the robot system controller to compensate the structural deflection, hence, minimizing the repeatability errors. This is more advantageous than increasing the thickness and size of the robot structure to stiffen the structure (Derby, 1983).

Mott (1999) has recommend an acceptable deflection ranges for machine member or a frame design, which is based on the machine application or requirement such as:

Due to bending	Deflection unit per length (m/m)
General	0.0005 to 0.003 m/m
Moderate precision	0.00001 to 0.0005 m/m
High precision	0.000001 to 0.00001 m/m

From the recommendation, robotic structure is considered as a high precision machine. For example, a lower arm structure overall length of 0.6m can only have an allowable maximum deflection of 0.006mm. However, in general at this deflection range, a design structure backlash can still occur. In the case of a bulky structure design, requirement to stiffen the structure to meet the maximum deflection could be overcome by utilizing composite material with high specific stiffness.

Adoption of computer aided engineering (CAE) in robot arm structure design process has increase the design process progress and efficiency. CAE is a finite element approach (FEA) computer application for general tasking encountered in mechanical engineering such as design, analysis and production (Mish & Mello, 2005). The CAE tool in robot structure design has been widely adopted for purpose of robot arm structure. Crytser, Nande and associates (Crytser, 1995) have been adopting ANSYS a CAE tool to design, stimulating, and sizing the proper pre-design properties for manipulator-coupled spacecraft. Others like Wang and Zhao (Wang & Zhao, 1993) has effectively used an ANSYS base programming language to optimize a robot structure with automatically design model modification.

ROBOT ARM DESIGN DETAIL

A robot arm has been designed for the purpose of arc welding application as shown in Figure 1. It has the workspace envelope of 1.3m radius with the maximum payload of 6kg at the wrist joint center. For a 6kg payload robot is categorized as a middle weight type robot arm, comparing with the existing industrial robot, it is objectively designed to achieve a repeatability error of ±0.1mm. At this stage of design specification, we are assuming that the robot arm repeatability error is totally due to the lower and upper arm linkage deflection. The distribution of the linkage structures deflection is distributed according to the sum of acting load to the linkages. A preliminary robot arm deflection distribution analysis is tabulated in Table 1.

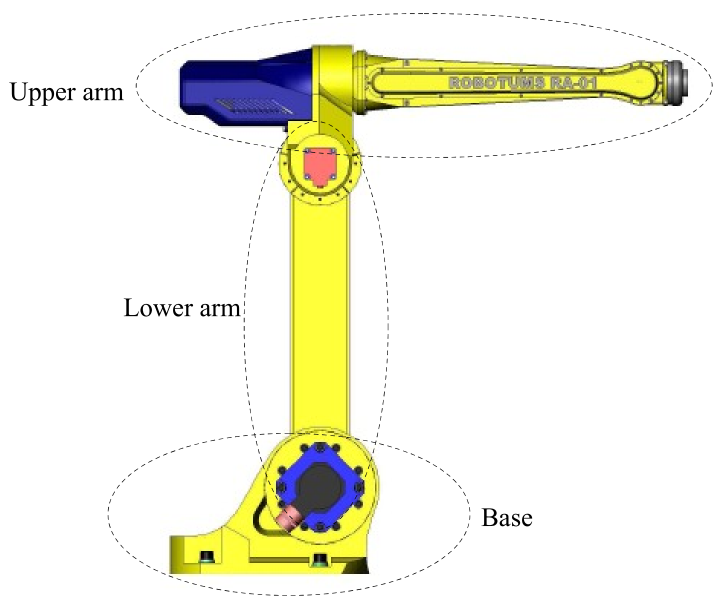

Figure 1. 3DOF articulated robot arm.

Table 1. Robot arm deflection distribution.

Linkage	Loading, P_i (N)	$P_i / [P_{UA} + P_{LA}]$	Deflection estimation, $\delta = \left[P_i / [P_{UA} + P_{LA}] \right] \times 0.1$ (mm)
Upper Arm	60	60/300 = 0.2	=0.2(0.1) = 0.02mm
Lower Arm	240	240/300=0.8	=0.8(0.1) = 0.08mm

MATERIAL MODELING AND SELECTION

Selection of a proper material type for a structure depends to the design requirement and material properties to suit its functionality. The structural performance is dependent on the combination of structure and properties (Ashby & Cebon, 1993). The strength and stiffness mechanical properties are the prime criteria for the lower arm structure. Other than the criteria of mechanical properties, cost, manufacturing method availability and machinability are also matters concern. Material such as aluminum alloy cast 319, steel AISI 1040, and malleable cast iron are an option.

Deflection Due To Pure Bending

The lower arm structure is an open end linkage, which can be modeled as a simple cantilever with end load (Figure. 2). Axial loading at the two ends can be ignored. Axial loading will only be occurred if the robot arm is configured to create compressive force at the end-effector.

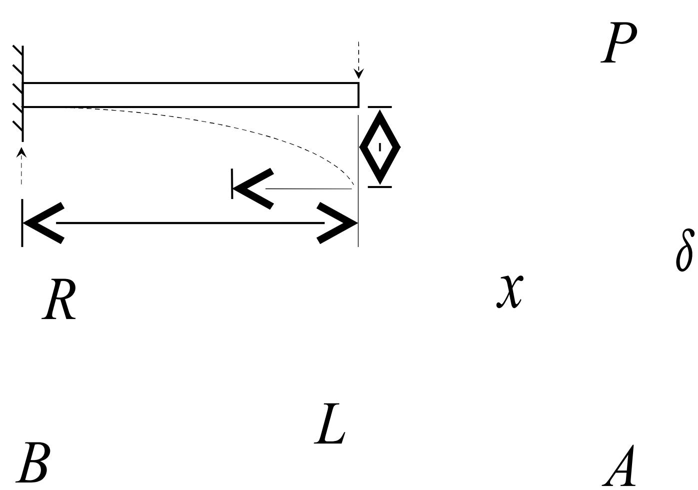

Figure 2. Cantilever structure

Simplified schematic representation of B is the close end that attached to the base through the shoulder joint, and A is the open end connecting to the upper arm with the elbow joint. The acting load P simulates the robot arm designed payload and the total weight of the upper arm including the wrist mechanism. The bending moment arises as the load is act upon the open end of the structure, which is defined by,

$$M = -PL \tag{3}$$

Substitute the bending moment equation (3) into equation (2) yields,

$$EI\frac{d^2\delta}{dx^2} = -Px \tag{4}$$

The cantilever deflection, δ is determined by solving the equation with two boundary conditions, when $\frac{d\delta}{dx} = 0$ at $x = L$ and when $\delta = 0$ at $x = L$. Such that,

$$\delta = \frac{P}{6EI}(-x^3 + 3L^2x - 2L^3) \tag{5}$$

The structure cross-section dimension is an influencing parameter in the deflection equation (5) and I-shape cross-section is considered due to it advantage of deflection resistance.

The moment inertia of I-section, Fig. 3, is define by,

$$I_{xx} = \frac{ab^3 - d^3(a-t)}{12} \tag{6}$$

By rewriting the deflection equation (5) and upon substituting equation (6) into it yields,

$$\delta = \frac{2P}{E}\frac{(-x^3 + 3L^2x - 2L^3)}{ab^3 - d^3(a-t)} \tag{7}$$

The maximum deflection will occur when $x = 0$,

$$\delta_{\max} = -\frac{4PL^3}{E}\frac{1}{ab^3 - d^3(a-t)} \tag{8}$$

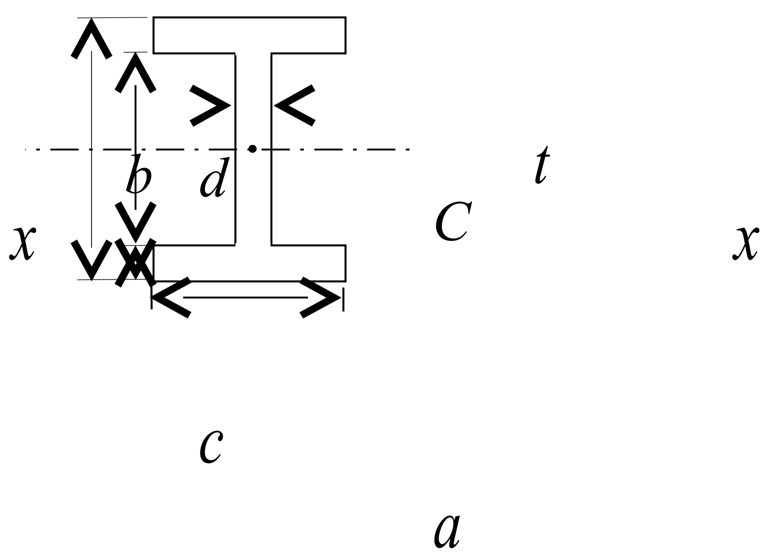

Figure 3. I-section properties

PRELIMINARY STRUCTURE DESIGN

The total loading of P in Figure. 2 with design factor of 1.5 is 440N acting at the free end of the cantilever. The lower arm structure deflection is determined by substituting the structural dimension and material properties into equation (8). The cross-section dimension and the type of material identification can be demonstrated by a flow chart shown at Figure 4.

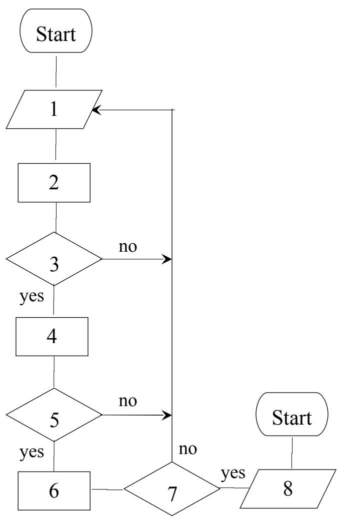

Input
dimension parameters
(a, b, c and t)
- material properties
(E and ρ)
Compute volume, mass and moment inertia.
Compare and .
Compute deflection.
Compare.
Compute.
Compare.
Store identified data.

Figure 4. Lower arm cross-section structure dimension and material identification process.

Material such as aluminum alloy cast 319, alloy steel 1040, and malleable cast iron are applied into the trial. The material type with the highest stiffness is selected and listed in the Table 2 below. The shear, moment and deflection diagram of each candidates are shown in Figure 5, Figure 6 and Figure 7.

Table 2. Material Type for Lower Arm Structure Design.

Dimension properties (mm)					Volume, V (m3)	Mass, m (kg)	Moment inertia, I (m4)	Deflection, δ (mm)	Stiffness, $k = \frac{P}{\delta}$ (N/mm)
a	B	c	d	t					
Candidates 1: Alloy Steel 1040 (E = 210GPa □=7700kg/m3)									
40	110	6	98	10	8.76E-4	6.745	2.0834E-6	0.073	6077.419
Candidates 2: Aluminum Alloy Cast 319 (E = 80GPa □=2790kg/m3)									
40	124	13	98	24	2.035-3	5.678	5.1E-6	0.0776	5667.21
Candidates 3: Malleable Cast Iron (E = 190GPa □=7300kg/m3)									
40	110	6	98	12	9.936E-4	7.253	2.24E-6	0.0744	5912,57

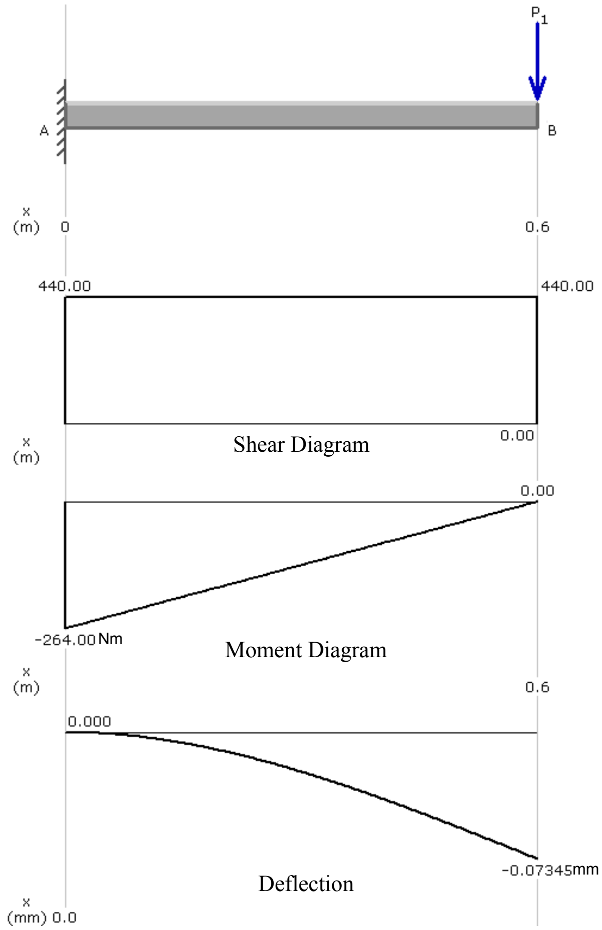

<u>Candidate 1 Alloy Steel 1040</u>

Figure 5. Shear, moment and deflection diagram of Material Type-1 (Alloy Steel 1040).

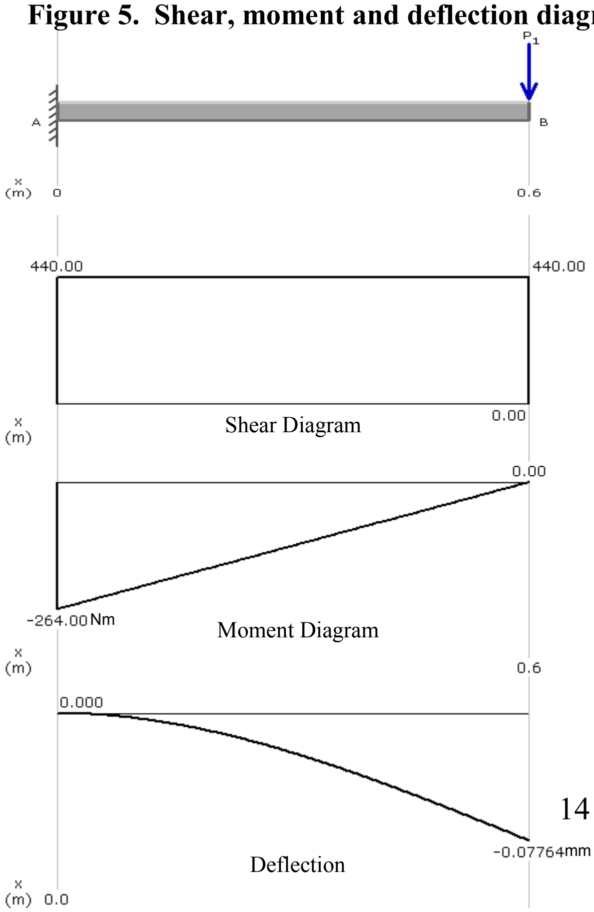

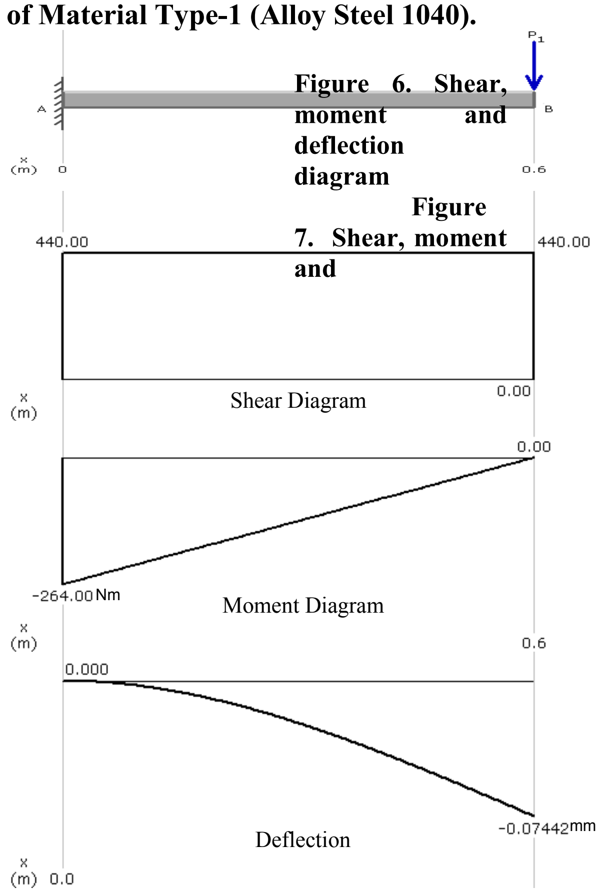

Figure 6. Shear, moment and deflection diagram

Figure 7. Shear, moment and

deflection diagram

***For Material Type-2 (Al-Alloy Cast 319).** *** For Material Type-3 (Malleable Cast Iron).**

LOWER ARM STRUCTURE VIRTUAL PROTOTYPE

Three virtual prototypes are constructed according to the candidate dimensions and type of materials by using Solidworks computer aided tool. Figure 8 illustrates the lower arm structure virtual prototype. Both of the structure ends is designed with a housing for the joint driving mechanism will be connected with an ‘I’ shape cross-section structure. The cross-section dimension of ‘I’ structure are modeled base on the identified dimension through theoretical approach that been proceed at the earlier stage.

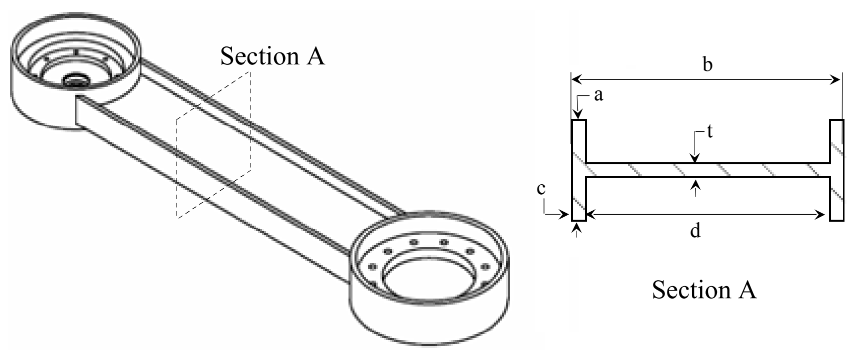

Figure 8. Lower Arm Structure Prototype.

CAE ANALYSIS AND RESULT

A CAE tool, CosmosWorks is applied to stimulate the designed lower arm structure model working condition to predict the behavior of the structure. Characteristic behavior such as stress and strain occurrence, displacement and deformation, and design failure under Von Mises stress, are virtually developed under static analysis through CosmosWorks. The CosmosWorks computation identifies the suitable structural dimension, and the type material for the lower arm structure to meet the constraint specification.

In this design task, static analysis is proceed to identify the preferable material and dimension for the lower arm structure. Displacement in the z-axis result will be monitor as the deflection of the structure. A 440N force acting along the z-axis direction is applied on the outer surface of housing A and fixed restraint point is place at twelve screw holes at housing B as shown in Figure 9.

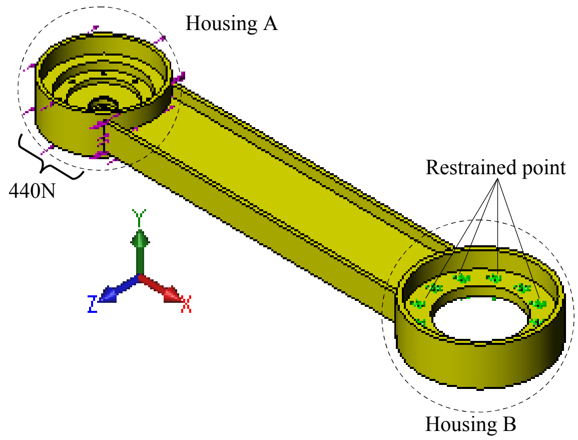

Figure 9. Acting forces and restrained point

Solid mesh type is applied to mesh the model for generating the nodes and elements. For the three types of materials used in this computation, alloy steel 1040 provided the best minimum deflection of 0.0705mm, followed by malleable cast iron (0073mm) and aluminum alloy 319 (0.095mm), with respect to decreasing stiffness (Table 3).

Table 3. Maximum deflection & stiffness of each material type through static displacement(z-axis) analysis.

No.	Material	Structure weight (kg)	No. of nodes	Deflection		Stiffness $k = P/\delta$ (N/mm)
				Max. (mm)	Node	
1.	Alloy Steel 1040	11.78	24411	0.0705	15009	6241.13
2.	Malleable Cast Iron	11.79	22264	0.073	7561	6027.4
3.	Aluminum Alloy 319	6.68	22606	0.095	2202	4631.6

Therefore, alloy steel 1040 provide best choice of material compared to the others. The computational deformation behavior of the lower arm structure for each type of material is also illustrated in the Figure 10. Static displacement analysis result of each material type-1, -2, and -3 are generated and illustrated in the following.

The analysis has shown the predicted behavior of a cantilever structure under an open-end loading for each material selection. All three models have the same maximum deflection occurrence location. Upon comparison of performance and material characteristics, alloy steel 1040 is the most suitable amount the others. Alloy steel 1040 structure has the highest stiffness, which is able to enhance the whole system efficiency and reducing the repeatability error to ±0.0705mm, provided the system accuracy is not affected by the joint actuators stiffness.

In comparing the FEA result (Table 3) with theoretical result (Table 2), the result of alloy steel 1040 and malleable cast iron have converged well. Except for the aluminum alloy cast 319, which deviates by about 28% attributed to the thickness of the housing A.

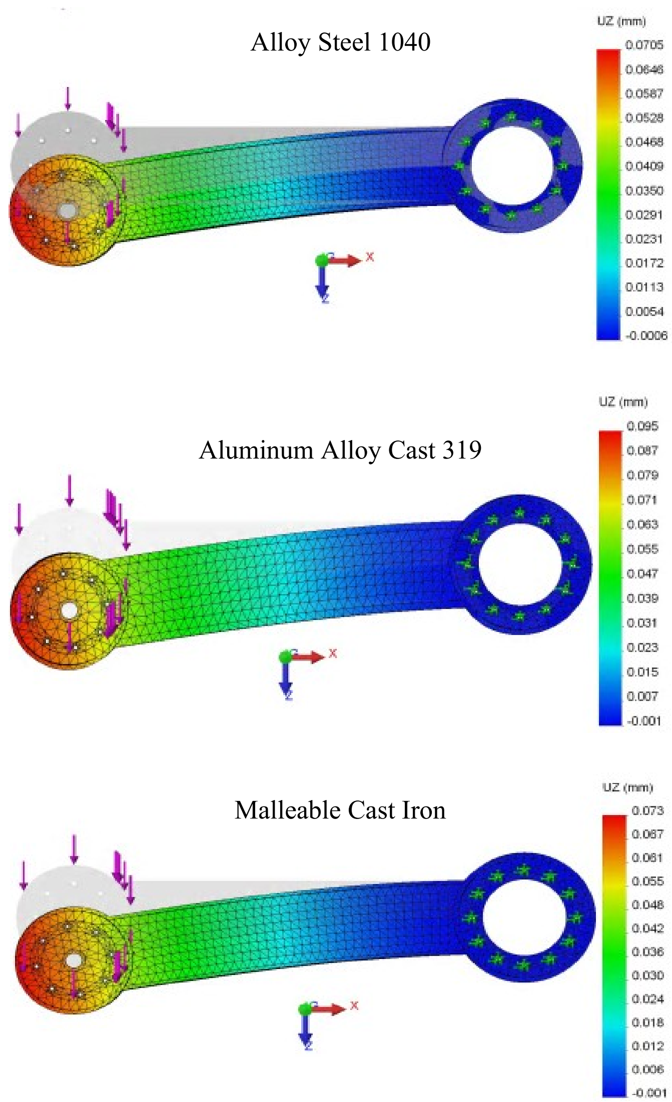

Figure 10. Static displacement (z-axis) analysis result.

CONCLUSION

The introduced approach of the dimension and material identification has improved and enhanced the lower structure design process efficiency and reduces the development time. The selected material type of alloy steel 1040 with the dimensional properties are able to reduce the robot arm repeatability error to about ±0.0705mm. The lower arm structure with complex geometric shape has been effectively simulated and analyzed through CosmosWorks to identify the appropriate type of material and structure cross-section dimension.

ACKNOWLEDGEMENT

The authors of this research project would like to acknowledge the supervision and support of the Centre of Materials & Minerals - CMM (Material Handling Technology Group), Universiti Malaysia Sabah.

REFERENCE

Ashby, M. F. & Cebon, D., 1993. *Material Selection in Mechanical Design*. Troisime Conference Europeenne sur les Materiaux et les Procedes Avances Euromat,.

Crytser, T., Nandi, G. C., Hinman-Sweeney, E. M., Dwivedi, S. N., Tobbe, P. A. & Lyons, D. W., 1995. Finite Element Design of Manipulator-Coupled Spacecraft for a Research Testbed. *Journal of Intelligent and Robotic Systems, Kluwer Acadamic Pub, Netherlands*, **13**:75-91.

Derby, S., 1983. The Deflection and Compensation of General Purpose Robot Arms. *Mechanism and Machine Theory*, **18**: 445-450.

Groover, M. P., 2000. *Automation, Production Systems and Computer-Integrated Manufacturing, Prentice Hal*l, New Jersey,.

Kim, Y. G., Jeong, K. S., Lee, D. G. & Lee, J. W., 1996. Development of the Composite Third Robot Arm of the Six-Axis Articulated Robot Manipulator. *Composite Structure*, **35**: 331-342.

Lewis, F. L., Fitzgerald, J. M., Walker, I. D., Cutkosky, M. R., Hurmuzlu, Y. & Nwokah, O., 2005. Robotics. Ed. Kreith, F. and Goswami, Y. *Handbook of Mechanical Engineering 2nd Edition*, CRC Press, Boca Raton,.

Mish, K. D. & Mello, J., 2005. *Computer Aided Engineering*. Ed. Kreith, F., Handbook of Mechanical Engineering, CRC Press, Boca Raton,.

Mott, R. L., 1999. *Machine Elements in Mechanical Design*. Prentice-Hall, New Jersey,.

Schilling, R. J., 1990. *Fundamentals of Robotics Analysis and Control*. Prentice Hall, New Jersey,.

Wang S., & Zhao J., 2002. FEM Optimization for Robot Structure. *IEEE Industrial Technology*, **Vol.1**: 510-513.